AIAA JOURNAL
Vol. 44, No. 7, July 2006

Novel Approach to Self-Sensing Actuation for Semi-Active Vibration Suppression

Kanjuro Makihara,* Junjiro Onoda,† and Kenji Minesugi‡
Japan Aerospace Exploration Agency, Kanagawa 229-8510, Japan

DOI: 10.2514/1.16018

A novel self-sensing method using piezoelectric actuators for semi-active vibration suppression is proposed and investigated. By using extended system equations, this self-sensing method can be implemented with a Kalman filter instead of the conventional bridge circuit technique. The method separates electrical status into two cases concerning electrical current, and characterizes each of these to establish the self-sensing system. This method is applicable to multiple-degree-of-freedom structures with multiple piezoelectric actuators. A numerical vibration suppression simulation demonstrated that the self-sensing method works well on a truss structure and has significant robustness against parameter variations. Experimental results also demonstrated that the self-sensing method suppresses not only single-mode vibration but also multiple-mode vibration.

Nomenclature

$\mathbf{B}_p$	=	input matrix
b_p	=	piezoelectric constant of piezoelectric actuator
C_p	=	constant-elongation capacitance of piezoelectric actuator
$\mathbf{C}_p$	=	diagonal capacitance matrix
k_p	=	constant-charge stiffness of piezoelectric actuator
I_{rms}	=	performance index for vibration suppression, Eq. (24)
$\vec{Q}$	=	charge vector composed of Q_j
Q_j	=	electric charge supplied to jth piezoelectric actuator
$\vec{Q}_T$	=	target charge vector obtained from active control
Q_{Tj}	=	target charge for jth piezoelectric actuator
u_1, u_2	=	x-directional displacements at tip and central nodes
$\vec{V}$	=	voltage vector composed of V_j
V_j	=	voltage across jth piezoelectric actuator
V^n	=	n-step voltage for discrete systems
$\mathbf{V}_1$, $\mathbf{V}_2$	=	noise intensity matrices for Eqs. (13) and (14), respectively
$\mathbf{W}_1$, $\mathbf{W}_2$	=	weighting matrices, Eq. (11)
$\vec{w}$	=	external force vector
$\vec{z}$	=	state vector, Eq. (7)
$\vec{z}_e$	=	extended state vector, Eq. (15)
Δt	=	time step for experimental hardware and simulation of self-sensing observer
δ_{rms}	=	root mean square of displacements of all truss nodes
ζ	=	modal damping coefficient
θ_{IIR}	=	IIR filter coefficient
$\vec{\xi}$	=	modal displacement vector
$\vec{\phi}_k$	=	eigenvector of kth vibration mode
ω_k	=	angular frequency of kth vibration mode

Subscripts and Superscripts

e	=	value for extended system
j	=	jth piezoelectric actuator or electric circuit (for L, Q, Q_T, R, V)
p	=	piezoelectric actuator
$\hat{\cdot}$	=	estimated value based on Kalman filter
$\bar{\cdot}$	=	smoothed value based on IIR filter

I. Introduction

FEEDBACK vibration controls need to know the state of a vibrating structure such as its modal displacements and velocities. Common vibration controls require structures to be equipped with sensors such as displacement or velocity sensors, strain gauges, accelerometers, and so forth. For large isolated structures such as a space station, installing various sensor equipment on many structural parts is impractical. Therefore, when it comes to vibration controls using piezoelectric actuators [1,2], it would be desirable if the state of the structure could be sensed by using a piezoelectric actuator as a sensor. A great number of researches on self-sensing methods of piezoelectric actuators have been conducted, and the use of a bridge circuit connected to a piezoelectric actuator is a common approach [3–7]. However, the high sensitivity of the bridge circuit to variations in the parameter values is a serious drawback of this technique. According to Anderson et al. [3], a mere 1% variation in piezoelectric capacitance can make active self-sensing control systems unstable because of the imbalance of the bridge circuit. These self-sensing approaches have been investigated intensively for the active vibration control.

Recently, some works on semi-active vibration suppression with piezoelectric actuators have been reported [8–18]. Clark [8] proposed a state-switching method implemented with a switchable stiffness element composed of a piezoelectric material. Cunefare et al. [9], Holdhusen and Cunefare [10], and Larson and Cunefare [11] proposed a state-switched vibration absorber to avoid potentially undesirable mechanical transients. Richard et al. [12,13] proposed a method to suppress vibration semiactively by

Received 9 February 2005; revision received 9 February 2006; accepted for publication 4 March 2006.

*Aerospace Project Research Associate, Department of Space Structure and Materials, Institute of Space and Astronautical Science, 3-1-1 Yoshinodai, Sagamihara; kanjuro@svs.eng.isas.jaxa.jp. Member AIAA.

†Professor, Department of Space Structure and Materials, Institute of Space and Astronautical Science, 3-1-1 Yoshinodai, Sagamihara. Associate Fellow AIAA.

‡Associate Professor, Department of Space Structure and Materials, Institute of Space and Astronautical Science, 3-1-1 Yoshinodai, Sagamihara. Member AIAA.

controlling a switch in a shunt circuit, which made good use of the passive energy-dissipation mechanism of a resistor. To improve this suppression performance, Richard et al. [14], Corr and Clark [15–17], and Onoda et al. [18] proposed another semi-active vibration suppression method using an inductive circuit. A piezoelectric actuator is shunted to the circuit for a short time in synchronization with the vibration. Corr and Clark [17] implemented multiple-mode vibration suppression based on the variable-stiffness control method [19]. Onoda et al.'s method [18] can suppress multiple-mode vibration by suppressing selective vibration modes, by using the control value obtained from a modern feedback active control. This energy-recycling approach was analyzed from the viewpoint of energy flow [20] and has been applied to various engineering applications [21].

In these semi-active studies, a piezoelectric actuator was connected to a passive electric circuit having a switch, instead of the voltage supplier that is commonly used for active vibration controls. The circuit switch is closed or opened to suppress the vibration of a structure. With most of these semi-active switching logics [12–18], electric current flows in the circuit only for a short time, and the circuit is open for most of the time. Therefore, in these semi-active vibration controls, it may be easier to sense the state of the structure by using a piezoelectric actuator than in active controls. A system that has only a single actuator and has to suppress single-mode vibration is called a single-input-single-output (SISO) system. For a SISO system, it is theoretically possible to implement semi-active vibration suppression by using the polarity of the voltage-rate (time difference of voltage) across the piezoelectric actuator as a control reference. However, switch-controlled semi-active methods sharply change the electric charge and voltage, like bang-bang type active controls do. That is, uncontrolled (or residual) modes are excited, whereas controlled modes are suppressed. The voltage-rate can thus be easily disturbed by the residual modes, which leads to the control systems malfunctions even if filtering techniques are used. Therefore, we have sought a new self-sensing method that is applicable to multiple-input-multiple-output (MIMO) systems, is less subject to the residual modes' influence, and does not need the sensitive bridge circuit technique.

This paper describes an innovative method of sensing the state of a vibrating structure by using a piezoelectric actuator in the energy-recycling semi-active vibration suppression method proposed by Onoda et al. [18] Although our previously proposed method [18] can suppress various vibrations, it still needs to have many sensors distributed across a structure. In contrast, our newly proposed self-sensing method uses extended system equations and a Kalman filter, instead of distributed sensors or bridge circuits. Compared with the conventional bridge circuit and simple voltage-rate self-sensing methods, our self-sensing method has the following advantages: 1) it can control multiple-mode vibrations by selectively suppressing vibration modes, because modal displacements and velocities can be estimated with the Kalman filter; 2) sufficient modal information keeps the self-sensing control system away from the harmful influence of residual modes; 3) it is much less sensitive to variations in parameter values; and 4) it can control multiple actuators cooperatively (in the sense of the centralized-control) rather than independently.

Our previous method [18] realizes these advantages by using several sensors. However, our newly proposed method also realized these advantages, not by using sensors, but by using a self-sensing approach. Thus, one can say that this proposed self-sensing method takes over the advantages that the previous method insisted on. In other words, the proposed self-sensing method is more advanced, and at the same time, includes the previous method. To clarify these advantages of our newly proposed self-sensing method, numerical simulations and experiments with a multiple-degree-of-freedom (MDOF) truss structure were conducted.

II. Self-Sensing Method for Semi-Active Vibration Suppression

In this work, the state of a vibrating structure is sensed by using a piezoelectric actuator functioning also as an actuator in the semi-active vibration suppression method proposed by Onoda et al. [18] Although this basic idea and procedure of implementation were described in our previous paper, a brief explanation is offered here for a better understanding of what follows.

A. Energy-Recycling Semi-Active Vibration Suppression

As an example of an MDOF system, let us consider an l-DOF truss structure having m piezoelectric actuators as shown in Fig. 1. Each actuator is described with four parameters: tensile load f, elongation u, voltage V, and electric charge Q as

$$f = k_p u - b_p Q, \qquad V = -b_p u + \frac{Q}{C_p} \tag{1}$$

where k_p, b_p, and C_p are functions of the characteristics of the piezoelectric actuator [18,22]. The equation of motion for the truss in modal coordinates is expressed as

$$\ddot{\vec{\xi}} + \mathbf{\Xi}\dot{\vec{\xi}} + \Omega\vec{\xi} - \mathbf{\Phi}^T\mathbf{B}_p\vec{Q} - \mathbf{\Phi}^T\vec{w} = 0 \tag{2}$$

and the voltage equation is written as

$$\vec{V} = -\mathbf{B}_p^T\mathbf{\Phi}\vec{\xi} + \mathbf{C}_p^{-1}\vec{Q} \tag{3}$$

where

$$\mathbf{\Phi} \equiv \left[\vec{\phi}_1, \vec{\phi}_2, \cdots, \vec{\phi}_l\right], \qquad \mathbf{\Omega} \equiv \text{diagonal}\left[\omega_k^2\right] \qquad \mathbf{\Xi} \equiv \text{diagonal}\left[2\zeta\omega_k\right] \tag{4}$$

Equations (2) and (3) can be transformed into

$$\dot{\vec{z}} = \mathbf{A}\vec{z} + \mathbf{B}\vec{Q} + \mathbf{E}\vec{w} \tag{5}$$

$$\vec{V} = \mathbf{C}\vec{z} + \mathbf{D}\vec{Q} \tag{6}$$

where

$$\vec{z} \equiv \left[\vec{\xi}^T, \dot{\vec{\xi}}^T\right]^T \tag{7}$$

$$\mathbf{A} \equiv \begin{bmatrix} \mathbf{0} & \mathbf{I} \\ -\mathbf{\Omega} & -\mathbf{\Xi} \end{bmatrix}, \qquad \mathbf{B} \equiv \begin{bmatrix} \mathbf{0} \\ \mathbf{\Phi}^T\mathbf{B}_p \end{bmatrix}, \qquad \mathbf{C} \equiv \begin{bmatrix} -\mathbf{B}_p^T\mathbf{\Phi} & \mathbf{0} \end{bmatrix} \tag{8}$$

$$\mathbf{D} \equiv \mathbf{C}_p^{-1}, \qquad \mathbf{E} \equiv \begin{bmatrix} \mathbf{0} \\ \mathbf{\Phi}^T \end{bmatrix} \tag{9}$$

Equation (5) indicates that well-developed linear control theories could be applied, if $\vec{Q}$ is directly controlled, for example, by using an electric charge supplier. In linear quadratic regulator (LQR) control theory [23], $\vec{Q}$ is controlled as follows:

$$\vec{Q} = \vec{Q}_T \equiv -\mathbf{K}\vec{z} \tag{10}$$

so that the performance index

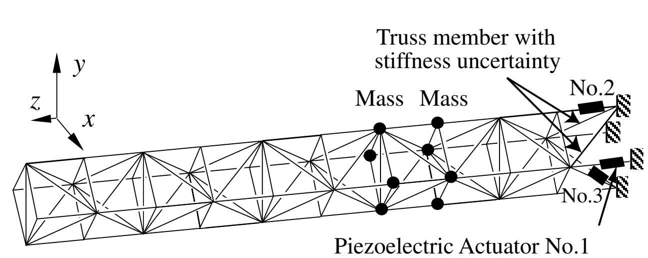

Fig. 1 Example of MDOF structure: 10-bay truss structure with three piezoelectric actuators.

$$J \equiv \int_0^\infty \left(\vec{z}^T \mathbf{W}_1 \vec{z} + \vec{Q}^T \mathbf{W}_2 \vec{Q}\right) \mathrm{d}t \tag{11}$$

is minimized. Here, $\mathbf{K}$ is the feedback matrix determined in the standard LQR scheme. Not all of the l vibration modes of the structure are necessarily taken into account, and we can select n vibration modes to be suppressed and construct $\vec{z}$ with these selected modes.

In the energy-recycling semi-active method [18], $\vec{Q}$ is not controlled directly. Instead of controlling $\vec{Q}$ actively, the method uses an inductive circuit composed of a switch and two diodes (Fig. 2). The jth circuit ($1 \leq j \leq m$) has a resistor R_j and an inductor L_j. In the figure, the piezoelectric actuator is modeled as a capacitor and a voltage generator V_a caused by the piezoelectric effect. A circuit is connected to each of the m actuators. The switching strategy is to control the jth circuit switch so that the polarity of the electric charge Q_j in the jth piezoelectric actuator traces the polarity of the jth target charge Q_{Tj} in Eq. (10). The switching logic for the jth circuit is written as

$$\begin{aligned} &\text{when } Q_{Tj} < 0, \quad \text{turn the } j\text{th switch to point 1} \\ &\text{when } Q_{Tj} > 0, \quad \text{turn the } j\text{th switch to point 2} \end{aligned} \tag{12}$$

The energy-recycling semi-active method can handle a system with multiple-mode vibrations and multiple actuators, because a target charge $\vec{Q}_T$ can be obtained from an active control theory designed for MIMO systems. In this method, every time the jth switch changes its point, the polarity of Q_j is reversed to trace the polarity of Q_{Tj}. Then, electrical energy is stored to be used later on rather than being dissipated. When we can generally assume that the mechanical vibration frequency is much lower than the electrical frequency of the circuit, the electric current flows only for a short period. In the intervals between the switch point changes, the electric current does not flow in the circuit, i.e., $\dot{Q}_j = 0$. During these intervals, the mechanical energy of the vibrating structure is converted into electrical energy through the piezoelectric actuator and is stored in the actuator. In consequence, the electrical energy increases cumulatively and the system can recycle the energy for effective vibration suppression.

The fundamental ideas of control methods [14–18] are the same. Because the comparison of these control methods has already been discussed [18,20], this paper does not again address the control logic comparison.

In general, $\vec{z}$ in Eq. (5) can be estimated with an estimator (e.g., the Kalman filter [23]), if both the control input vector $\vec{Q}$ and the output measurement vector $\vec{V}$ can be measured. In contrast to active controls, the semi-active switching control does not know the $\vec{Q}$ value. Although it is theoretically possible to calculate $\vec{Q}$ by integrating electric current with time, it is actually impossible to obtain $\vec{Q}$ precisely, because of the rapid change of electrical state. Therefore, due to the lack of the $\vec{Q}$ value, the general Kalman filter estimation by using Eqs. (5) and (6) cannot be conducted. To implement a self-sensing control system, we have searched for a novel estimation method that does not need the $\vec{Q}$ measurement.

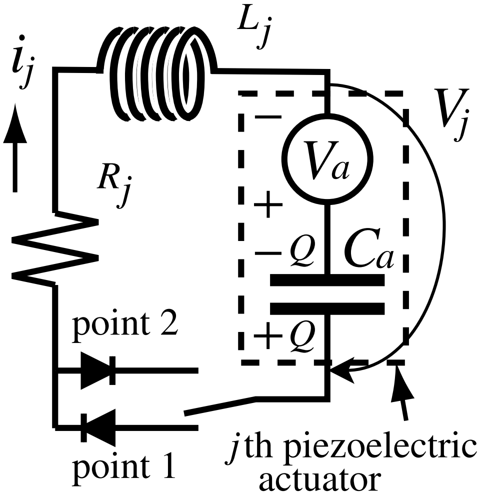

Fig. 2 Electric circuit for vibration suppression connected to jth piezoelectric actuator.

B. Novel Self-Sensing Method with Extended System

To obtain the value of $\vec{Q}_T$ in Eq. (10), the state of the structure $\vec{z}$ needs to be known. Conventional bridge circuit self-sensing methods usually have the problem of the system instability. Moreover, simple voltage-rate self-sensing methods are difficult to apply to MIMO systems and are subject to the residual modes' influence. Therefore, to overcome these disadvantages, we propose the novel self-sensing method using extended state equations and a Kalman filter [23].

As described earlier, the electric current flows in the circuit only for a short period in the energy-recycling semi-active method. This means that $\dot{\vec{Q}} = \vec{0}$ is valid most of the time. Therefore, we first discuss the case that $\dot{\vec{Q}} = \vec{0}$. In this case, Eqs. (5) and (6) can be transformed into

$$\dot{\vec{z}}_e = \mathbf{A}_e \vec{z}_e + \mathbf{E}_e \vec{w} \tag{13}$$

$$\vec{V} = \mathbf{C}_e \vec{z}_e \tag{14}$$

where

$$\vec{z}_e \equiv \left[\vec{z}^T, \vec{Q}^T\right]^T \tag{15}$$

$$\mathbf{A}_e \equiv \begin{bmatrix} \mathbf{A} & \mathbf{B} \\ \mathbf{0} & \mathbf{0} \end{bmatrix}, \qquad \mathbf{C}_e \equiv \begin{bmatrix} \mathbf{C} & \mathbf{D} \end{bmatrix}, \qquad \mathbf{E}_e \equiv \begin{bmatrix} \mathbf{E} \\ \mathbf{0} \end{bmatrix} \tag{16}$$

Equations (13) and (14) are referred to as the extended state and the extended output equations, respectively. The Kalman filter for estimating $\vec{z}_e$ is

$$\dot{\hat{\vec{z}}}_e = \mathbf{A}_e \hat{\vec{z}}_e + \Gamma_e\left(\vec{V} - \mathbf{C}_e \hat{\vec{z}}_e\right) \tag{17}$$

where Γ_e is defined as

$$\Gamma_e \equiv \mathbf{P}\mathbf{C}_e^T \mathbf{V}_2^{-1} \tag{18}$$

Here, $\mathbf{P}$ is a positive definite solution of

$$\mathbf{A}_e \mathbf{P} + \mathbf{P}\mathbf{A}_e^T - \mathbf{P}\mathbf{C}_e^T \mathbf{V}_2^{-1} \mathbf{C}_e \mathbf{P} + \mathbf{V}_1 = \mathbf{0} \tag{19}$$

As long as $\dot{\vec{Q}} = \vec{0}$, by updating Eq. (17) with the measured voltage $\vec{V}$, we can estimate the state vector $\hat{\vec{z}}$ by extracting it from the extended state vector $\hat{\vec{z}}_e$.

Next, let us consider the case that the electric current flows, i.e., $\dot{\vec{Q}} \neq \vec{0}$. Even in this case, it is theoretically possible to construct an observer based on the characteristics of the electric circuit, such as Kirchhoff equations. However, as stated, because the current varies very rapidly in actual systems, calculating the charge precisely by integrating the current is impractical. Therefore, for a short duration while the jth circuit current flows, from Eq. (6), Q_j can be estimated as

$$\hat{Q}_j = j\text{th element of } \mathbf{D}^{-1}\left(\vec{V} - \mathbf{C}\hat{\vec{z}}\right) \tag{20}$$

and $\hat{\vec{Q}}$ can be constructed from $\hat{Q}_j$. Elements of $\hat{\vec{Q}}$ other than the jth element have constant values. Because Eq. (13) is no longer valid, the state of the system can be estimated from Eq. (5) as

$$\dot{\hat{\vec{z}}} = \mathbf{A}\hat{\vec{z}} + \mathbf{B}\hat{\vec{Q}} \tag{21}$$

By using Eqs. (20) and (21) simultaneously, $\hat{\vec{z}}$ can be estimated.

In summary, for both $\dot{\vec{Q}} = \vec{0}$ and $\dot{\vec{Q}} \neq \vec{0}$, the state of the system can be estimated without $\vec{Q}$ measurement. Consequently, $\vec{Q}_T$ in Eq. (10)

can be obtained. The switch point can thus be determined with $\vec{Q}_T$, following the switching logic in Eq. (12).

There is another simple way of estimation when $\dot{\vec{Q}} \neq \vec{0}$. If we assume that the electric oscillation in the circuit is much faster than the mechanical vibration, the state of the structure $\hat{\vec{z}}$ can be assumed to be constant when $\dot{\vec{Q}} \neq \vec{0}$. Therefore, for a short duration while the electric current flows in the jth circuit, Q_j can be estimated from Eq. (20) with a constant $\hat{\vec{z}}$. Although this simple estimation method may reduce the calculation cost in practice, it will not be used in what follows.

Note that this proposed self-sensing method can select the vibration modes to be suppressed, and thus, selective multiple-mode vibration suppression is possible. Furthermore, our method can select the vibration modes to be estimated. Specifically, it is not necessary to construct the state vectors $\vec{z}$ in Eqs. (7) and (15) by using all vibration modes. Moreover, $\vec{z}$ in Eq. (7) can have different elements or a different dimension from $\vec{z}$ in Eq. (15). In actual systems, as in modal truncation, the several vibration modes are usually considered (or selected) to be suppressed or estimated. Each $\vec{z}$ is constructed with the selected modes for each requirement. There is ample flexibility to construct each vector $\vec{z}$ in Eqs. (7) and (15).

III. Numerical Simulation of Self-Sensing Vibration Suppression

To investigate how the novel self-sensing method works, numerical simulations were performed on the truss structure shown in Fig. 1. This 10-bay truss structure design was also used in the vibration suppression experiments that will be discussed later. The axial member weighed 35.7 g and the diagonal member weighed 46.3 g. Each node weighed 67.9 g. Each axial member had a stiffness of 1.99×10^6 N and a length of 0.38 m. The diagonal member had a length of $\sqrt{2}$ times that of the axial member and the same stiffness as the axial member. The values for the piezoelectric actuator defined in Eq. (1) were $k_a = 5.75 \times 10^6$ N/m, $b_a = 2.57 \times 10^5$ N/C, and $C_a = 1.17 \times 10^{-5}$ F. The damping ratio ζ of each mode was assumed to be 3.60×10^{-3}. Note that the damping ratio of the first mode in the simulation was exactly the same as the actual damping ratio in the experiment.

From the energy-recycling standpoint, the resistance in the circuit should be kept as low as possible [18,20]. However, in actual system, some resistance value in the circuit is inevitable. Furthermore, real piezoelectric actuators have an equivalent resistance. According to [24] piezoelectric actuators have the equivalent resistance that decreases with an increase in the cycle number of input sinusoidal voltage. Based on that research conclusion, the measurement of the actual piezoelectric actuator used in our experiment determined the total circuit resistance to be 3.98 Ω. There is usually an optimal inductance value for each semi-active system. After an iteration process, we set the inductance value as 2.23×10^{-3} H, which was the same as that for the experimental parameter.

The following simulation had a time step of 1.0×10^{-7} s, which was small enough compared with the highest mechanical vibration mode (whose period was 4.9×10^{-4} s) and the electrical oscillation (whose period was 1.0×10^{-3} s). On the other hand, the self-sensing observer expressed by Eqs. (17), (20), and (21) was updated every period of $\Delta t (= 3.0 \times 10^{-4}$ s), which was the time step of the experimental hardware.

A. Self-Sensing Vibration Suppression with a Single Actuator

We first simulated single-mode vibration suppression for the truss structure having a single piezoelectric actuator. This actuator was actuator number 1 of the structure as illustrated in Fig. 1. The lowest mode was sensed with the self-sensing method expressed by Eqs. (17), (20), and (21), and was controlled with the switching logic of Eq. (12). The initial modal velocity of the first mode was set to 0.01 $\mathrm{m \cdot kg^{1/2}/s}$ and its modal displacement was zero. The initial modal displacements and velocities of all the other modes were zero. $\hat{\xi}_1$, $\hat{\dot{\xi}}_1$, and $\hat{Q}$ had initial values of zero. To obtain $\vec{Q}_T$ in Eq. (10), LQR control theory was used. $\mathbf{W}_1$ in Eq. (11) was set to

$$\mathbf{W}_1 = \mathrm{diagonal}\left[1, \frac{1}{\omega_1^2}\right] \tag{22}$$

and $\mathbf{W}_2$ was set as a scalar W_2. $\mathbf{V}_1$ in Eq. (19) was given as

$$\mathbf{V}_1 = \mathrm{diagonal}[0, \alpha_1, \beta_1] \tag{23}$$

Because a single actuator was used, $\mathbf{V}_2$ was set as a scalar unit, i.e., 1. W_2, α_1, and β_2 were the design variables of the self-sensing method. During the self-sensing vibration suppression, the following integral was calculated as the performance measure:

$$I_{\mathrm{rms}} \equiv \int_{t_S}^{t_E} \delta_{\mathrm{rms}}\,\mathrm{d}t \tag{24}$$

where $t_S = 0.0$ s and $t_E = 0.5$ s. I_{rms} was not only a measure of vibration suppression of controlled modes, but also a measure of the influence of uncontrolled modes excited in every switching. With extensive parametric study, W_2, α_1, and β_1 were optimized as 1.0, 3.2, and 3.2×10^{-8}, respectively, such that I_{rms} was minimal.

Figure 3 shows time histories of single-mode vibration suppression with the self-sensing method. To see qualitatively how accurately $\hat{\xi}_1$ and $\hat{Q}$ were estimated, the corresponding exact values ξ_1 and Q are also presented in the figure. The first peak in the time history of $\hat{\xi}_1$ was lower than the exact value ξ_1. However, the estimation of the first mode and electric charge became accurate gradually after the self-sensing control started at $t = 0$. The value of $\vec{Q}_T$ was calculated with the estimated modal data, resulting in the appropriate switching signal. By switching between points 1 and 2 around the peak of the first modal displacement, the polarity of the electric charge was reversed. During the intervals of the switchings, the estimated electric charge was constant, exactly as the self-sensing method specified. The value of I_{rms} for the suppressed system was 3.2×10^{-6} ms, whereas I_{rms} with no control (i.e., free vibration) was 7.2×10^{-6} ms. Through this numerical simulation, it was confirmed

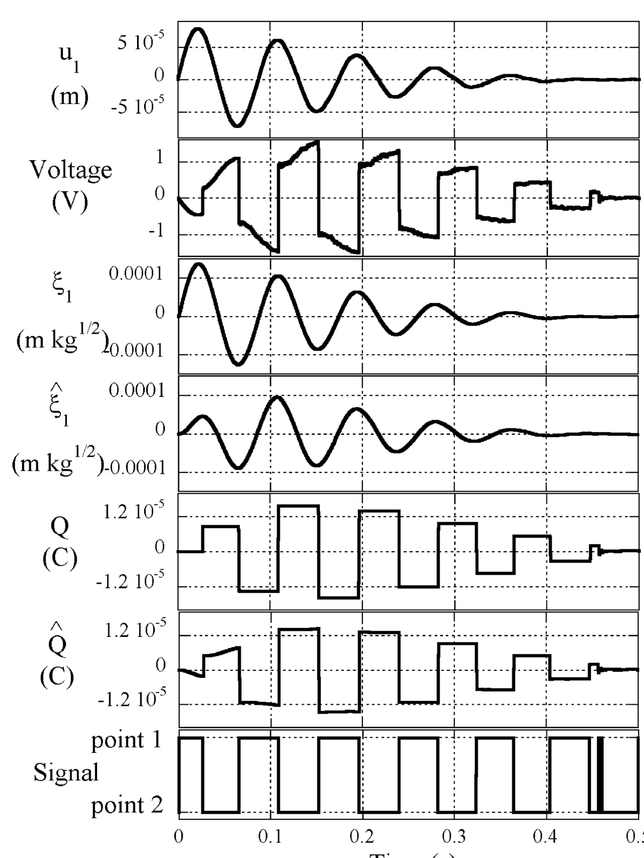

Fig. 3 Time histories of self-sensing single-mode vibration suppression.

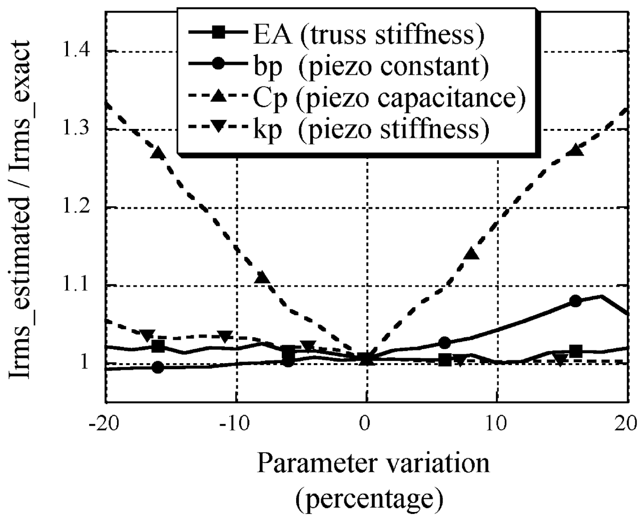

Fig. 4 Robustness of vibration suppression to intentional model errors.

that the self-sensing method worked well to suppress single-mode vibration.

B. Robustness of Self-Sensing Vibration Suppression

Regarding conventional self-sensing methods with bridge circuits, much attention has been paid to the robustness of the vibration suppression performance against parameter variation. Accordingly, the robustness of the proposed self-sensing method was investigated by conducting numerical simulations with intentional model errors. We used the same structure and actuator as in the last section. The initial conditions were also the same as the previous ones. First, we designed the self-sensing control system by using the optimal combination of weighting matrices that was previously determined in the first simulation. Next, after designing the control system, the stiffness EA of two truss members (Fig. 1 indicates the members with stiffness uncertainty) was varied by a factor of EA/EA_{nominal}, keeping all other parameters unchanged. In the simulations, the intentional model errors were caused by this EA variation. Here, E is the Young's modulus and A is the cross-sectional area of the truss member. In the self-sensing vibration suppression based on the estimated values $\hat{\xi}_1$ and $\hat{\dot{\xi}}_1$, the performance measure $I_{\mathrm{rms-estimated}}$ defined in Eq. (24) was calculated. Here, "estimated" means that vibration suppression was conducted by using $\hat{\xi}_1$ and $\hat{\dot{\xi}}_1$ obtained from the proposed self-sensing method. When EA deviated from its nominal value, the self-sensing estimation accuracy might deteriorate, and the structural properties (e.g., structural frequencies) also changed. Therefore, to separate the influences on the suppression performance by the deterioration of self-sensing estimation and by the change of structural properties, we also conducted a vibration suppression simulation using exact values ξ_1 and $\dot{\xi}_1$, instead of the self-sensing estimation, and calculated $I_{\mathrm{rms-exact}}$.

Figure 4 plots $I_{\mathrm{rms-estimated}}/I_{\mathrm{rms-exact}}$ as a function of EA/EA_{nominal}. The slope of the curve is quite gentle, meaning that the self-sensing system's performance did not deteriorate much due to model errors. We also conducted three similar simulations, varying piezoelectric constant b_p, piezoelectric capacitance C_p, and piezoelectric stiffness k_p in Eq. (1). Among these parameter variations, the piezoelectric capacitance variation had a relatively large influence on the self-sensing suppression performance. However, the self-sensing method was still more robust against model errors in comparison with conventional bridge circuit self-sensing methods.

C. Comparison with Voltage-Rate Self-Sensing Method using IIR Filter

When a structure is assumed to have only single-mode vibration, the voltage-rate (time difference of voltage) across the piezoelectric actuator is proportional to the modal velocity of this mode while the electric current does not flow. This can be confirmed easily when the equation $\dot{\vec{Q}} = \vec{0}$ is substituted into a time-derivative scalar equation obtained from Eq. (3). Therefore, for this simple system, self-sensing vibration suppression based on the voltage-rate is possible. This suppression was carried out with the measured voltage by Richard et al. [14] In this case, a switch in a circuit is closed when the voltage is at maximum, i.e., when the voltage-rate crosses the zero line. For convenience of explanation, this self-sensing method is referred to as a "voltage-rate method." The differences between our method and the voltage-rate method are described next.

First of all, it is clear that the voltage-rate method is hard to implement if the goal is suppressing selective multiple vibration modes. Next, the voltage-rate method can also be easily degraded by residual modes. The harmful influence of the residual modes when using the voltage-rate method was confirmed in numerical simulations. In these simulations, an infinite impulse response (IIR) filter [25] was used for digital low-pass processing. The IIR filter can achieve a given filtering characteristic using less memory and fewer calculations than a similar finite impulse response (FIR) filter can. In this sense, the IIR filter is desirable for real-time vibration controls. With the IIR filter, a smoothed voltage-rate is calculated as follows. First, the n-step measured voltage V^n is smoothed into $\bar{V}^n$ with the IIR filter. Next, the voltage-rate is calculated in the manner of time difference. Then, the voltage-rate $\dot{\bar{V}}^n$ is smoothed into $\bar{\dot{\bar{V}}}^n$ with the IIR filter. This procedure is

$$\bar{V}^n = \theta_{\mathrm{IIR}}\bar{V}^{n-1} + (1-\theta_{\mathrm{IIR}})V^n \tag{25}$$

$$\dot{\bar{V}}^n = (\bar{V}^n - \bar{V}^{n-1})/\Delta t \tag{26}$$

$$\bar{\dot{\bar{V}}}^n = \theta_{\mathrm{IIR}}\bar{\dot{\bar{V}}}^{n-1} + (1-\theta_{\mathrm{IIR}})\dot{\bar{V}}^n \tag{27}$$

where the bar indicates an IIR-filtered value. The voltage-rate self-sensing method changes the switching point according to the polarity of $\bar{\dot{\bar{V}}}^n$. When the polarity is positive, the switch is connected to point 2, whereas when it is negative, the switch is connected to point 1. The voltage-rate method is thus a simple case of the energy-recycling semi-active method. This switching logic for voltage-rate method is obtained by substituting $Q_{Tj} = \bar{\dot{\bar{V}}}^n$ and $j = 1$ into the switching logic expressed in Eq. (12). The voltage-rate method does not need modal information or structural model. However, though our self-sensing approach needs such information, it has several advantages over the voltage-rate method, as this paper described.

Figure 5 shows I_{rms} as a function of θ_{IIR}. The minimum I_{rms} was 4.2×10^{-6} ms, with an optimal coefficient θ_{IIR} of 0.89 (indicated with a filled circle in Fig. 5). Figure 6 shows time histories of vibration suppression using the voltage-rate method with the optimal coefficient value. After the control started at $t = 0$, the voltage-rate signal became rough because of the residual modes that were excited by the switching. Consequently, after $t = 0.24$ s, the control malfunctioned because of the rough voltage-rate data even with the smoothing IIR filter.

It should be noted that how the residual modes worsen control systems depends on the type of structure. A truss structure, which is a typical space structure, may be harmfully influenced by residual modes, because its residual modes are generally easy to excite and they linger longer, compared with beam and plate structures [14–17]. Here, we presented one case of vibration suppression on the truss structure by using the voltage-rate method with a simple IIR-filtering on the assumption that two coefficients in Eqs. (25) and (27) were the same for convenience. However, even if a more complicated filtering could be applied, the voltage-rate would not be likely to be smoothed enough to be used for the semi-active vibration suppression of the truss structure. A comparison of Figs. 3 and 6 clearly demonstrates that the proposed self-sensing method is far less sensitive to the residual modes' influence.

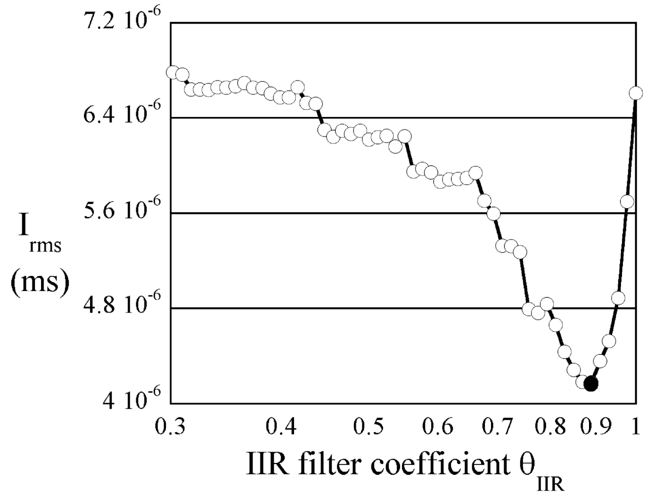

Fig. 5 Performance of self-sensing control based on IIR-filtered voltage-rate.

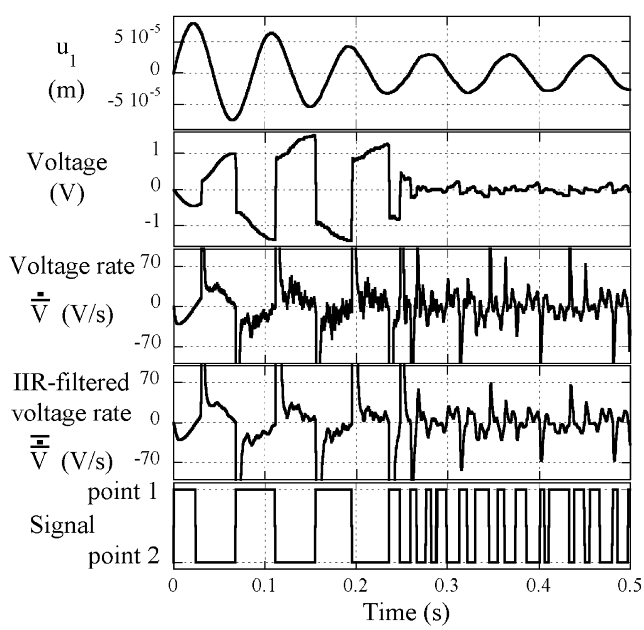

Fig. 6 Time histories of self-sensing control based on IIR-filtered voltage-rate ($\theta_{\mathbf{IIR}} = 0.89$).

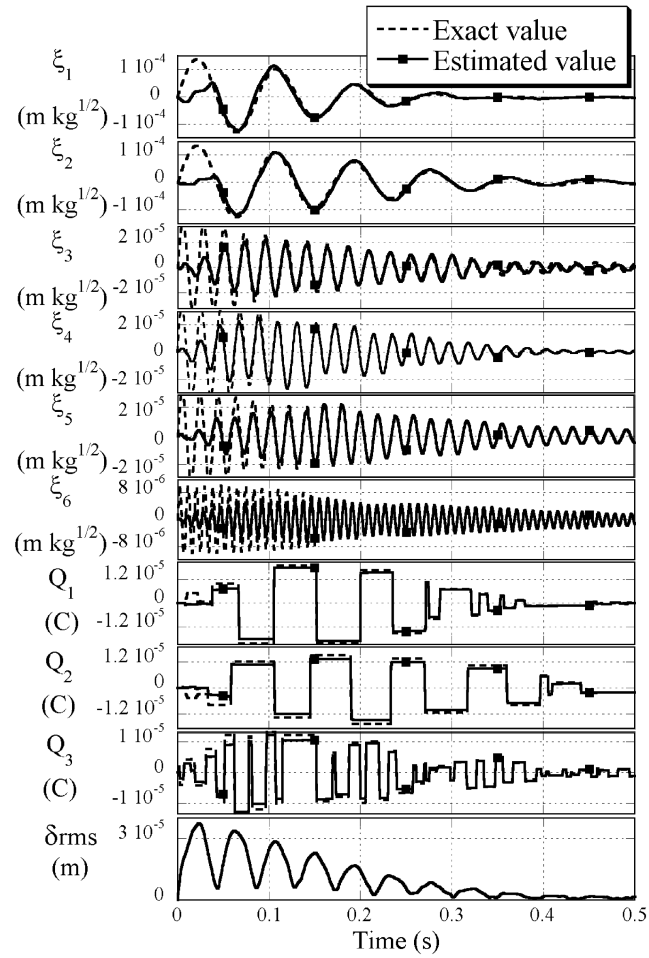

Fig. 7 Time histories of self-sensing six-mode vibration suppression using three piezoelectric actuators.

In contrast to the proposed self-sensing approach, it seems that one could develop a frequency-shaped controller to target individual modes. Their method does not need a model but requires band-pass filters around targeted modes. Specifically, the processor passes the piezoelectric voltage signals between the two specific frequencies, and finally detects the targeted modes. Whereas this approach is one alternative for the self-sensing vibration control, structural frequency information to set the two specific frequencies is still required. In conclusion, there are several alternatives to apply the self-sensing switching vibration control. Depending on the objectives and structures for vibration suppression, one can select the appropriate self-sensing approach.

D. Multiple-Mode Vibration Suppression with Multiple Actuators

To see whether the proposed self-sensing method was effective in suppressing the multiple-mode vibration of a system having multiple piezoelectric actuators, we simulated vibration suppression of a 10-bay truss structure with three piezoelectric actuators. The three actuators shown in Fig. 1 were the three actuators used for the MIMO system. For simplicity, the three actuators were assumed to be identical. The initial velocities of the lowest six modes were $0.01\ \mathrm{m\cdot kg^{1/2}/s}$ and their modal displacements were zero. The initial modal displacements and velocities of all the other modes were zero. All estimated values had initial values of zero. The excited free six-mode vibration was suppressed with three actuators. To obtain the value of $\vec{Q}_T$, the LQR control scheme was used. The weighting matrices in Eqs. (11) and (19) were approximately optimized as

$$\mathbf{W}_1 = \text{diagonal}\left[1, \cdots, 1, \frac{1}{\omega_1^2}, \cdots, \frac{1}{\omega_6^2}\right] \tag{28}$$

$$\mathbf{W}_2 = 1.0 \times 10^{-1}\text{diagonal}[1, 1, 1] \tag{29}$$

$$\mathbf{V}_1 = \text{block diagonal}[\mathbf{0}_6, 1.0 \times 10^1 \mathbf{I}_6, 1.0 \times 10^{-8} \mathbf{I}_3] \tag{30}$$

$$\mathbf{V}_2 = \mathbf{I}_3 \tag{31}$$

with which I_{rms} was minimal. Figure 7 shows time histories of suppressing six-mode vibration with the self-sensing method. The nine estimated values are compared with the corresponding exact values. The estimation of the first and the second modes became accurate after the control started at $t = 0$. Eventually, all six modes were estimated accurately enough to be used for semi-active vibration suppression. This result demonstrates that the self-sensing method can suppress the multiple-mode vibration of an MDOF structure and handle multiple piezoelectric actuators cooperatively in the sense of the centralized-control. Note that the number of the estimated and suppressed modes can be larger than the number of the actuators, which is another advantage of this self-sensing method.

IV. Self-Sensing Vibration Suppression Experiments

The self-sensing suppression experiments used the 10-bay cantilevered truss structure shown in Fig. 8. Because truss members at the base could not support the total weight of the structure, the structure was hung from the tip and the central nodes on strings that were 2.95 m long. This compensated for the weight, but restricted its motion to the x–z plane. Therefore, in the following experiments, only horizontal bending vibrations in the x–z plane were excited and suppressed. A commercially available NEC/TOKIN ASB171C801NP0 piezoelectric actuator was used, and it was installed at the truss base. It had a length of 0.22 m and a mass of 93.0 g and was composed of 1300 piezoceramic layers.

The control flow was as follows (see also Fig. 9). First, only the measured voltage of the actuator was sent through an analog-digital converter to a processor. Next, the processor estimated vibration modes and electric charge by using Eqs. (17), (20), and (21). Then, the processor calculated the target charge and, if necessary, sent a signal through a digital-analog converter to the switch. On receiving the signal, the switch would change its point. It should be emphasized that the self-sensing control system did not use the measured displacements of the tip node u_1 and the central node u_2 for vibration suppression, and these values were only measured as records.

A. Single-Mode Vibration Suppression

A single-mode vibration suppression experiment was performed to investigate whether the self-sensing method suppressed the vibration of an actual structure. The experimental system had the same weighting matrices as in the single-actuator simulation. The first horizontal bending mode (11.5 Hz) in the x–z plane was excited by using an exciter. After the excitation ceased, the subsequent free vibration was suppressed by using the self-sensing method. Figure 10 shows time histories of single-mode vibration suppression. Until the semi-active control started at $t = 0.9$ s, the self-sensing estimation worked and the electric circuit was opened so that electric current did not flow. After the self-sensing vibration suppression began, the first mode was still estimated accurately, in view of the time history of the tip displacement u_1. Consequently, the first-mode vibration was quickly suppressed in the following 0.35 s. The circuit switch changed its point around each peak of the estimated first mode. During the switching intervals, the estimated value of $\hat{Q}$ was constant, as the method required. This experiment proved that the self-sensing method could suppress single-mode vibration on an actual system.

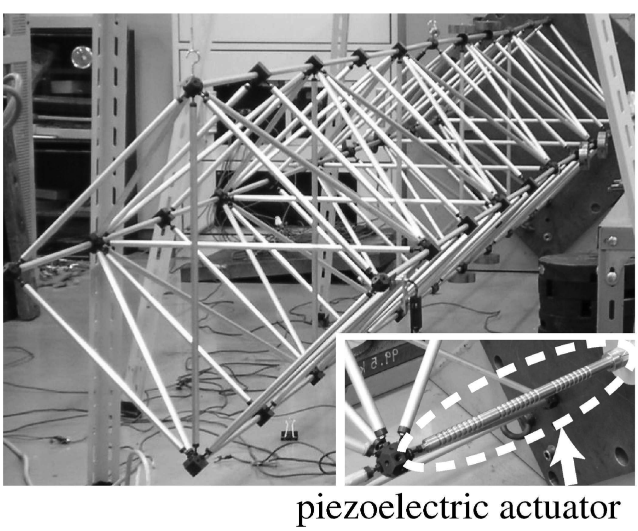

Fig. 8 Experimental setup for self-sensing vibration suppression experiments.

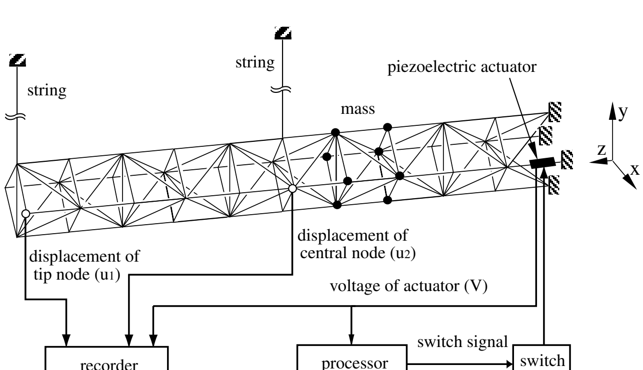

Fig. 9 Control flow of self-sensing vibration suppression experiment.

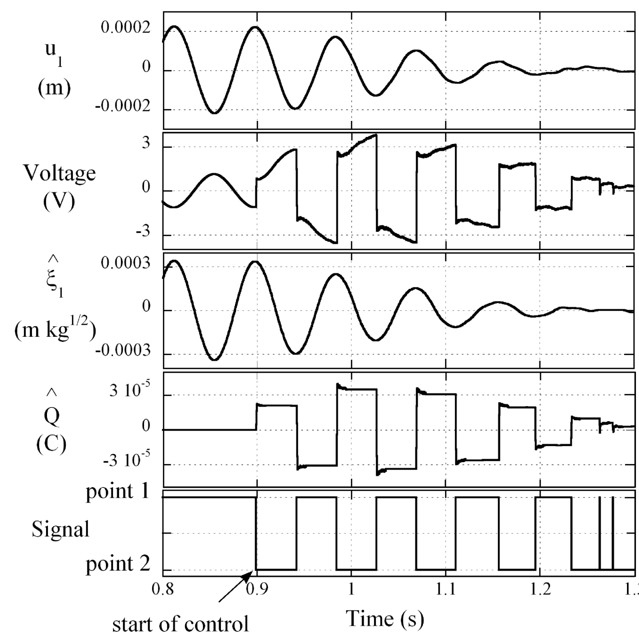

Fig. 10 Experimental result for single-mode vibration suppression.

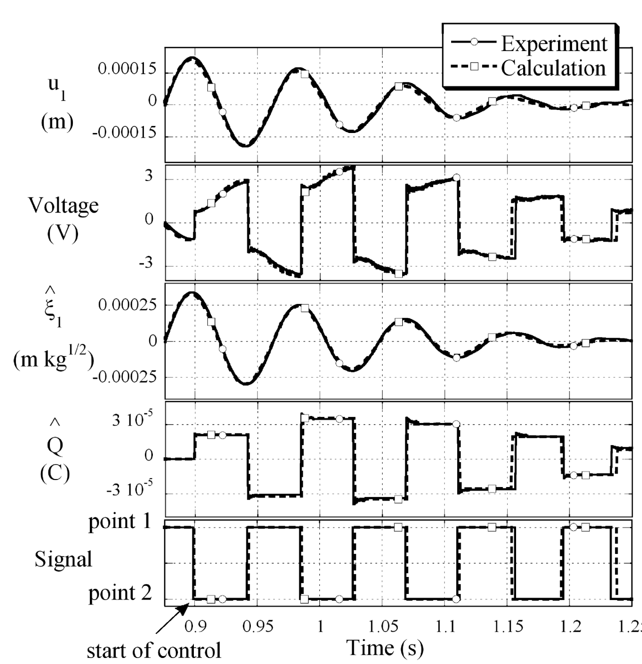

Fig. 11 Comparison of experimental result and numerical simulation result.

Figure 11 shows the comparison between the experimental result shown in Fig. 10 and the result numerically simulating the experiment. Note that the damping ratio of the first mode in the simulation was exactly the same as the actual damping ratio in the experiment. The simulation was started at $t = 0.88$ s, i.e., when u_1 and V approached zero. At this time, $\hat{\dot{\xi}}_1$ was given as $0.024\ \mathrm{m \cdot kg^{1/2}/s}$, and all other variables were set to zero. These initial values were obtained from the experimental result in Fig. 10. Both of the time histories are very similar to each other. This similarity indicates that the modeling of the system for numerical simulations is acceptable for the actual design of the proposed self-sensing method.

B. Multiple-Mode Vibration Suppression

A two-mode vibration suppression experiment was performed next. For the self-sensing control system, the weighting matrices were set as

$$\mathbf{W}_1 = \mathrm{diagonal}\left[1, 1, \frac{1}{\omega_1^2}, \frac{1}{\omega_2^2}\right] \tag{32}$$

$$\mathbf{V}_1 = \mathrm{diagonal}[0, 0, 3.2, 3.2, 3.2 \times 10^{-8}] \tag{33}$$

and $\mathbf{W}_2$ and $\mathbf{V}_2$ were set as scalar units. The lowest two horizontal bending modes (11.5 and 48.0 Hz) in the x–z plane were first excited using the exciter. After the excitation ceased, the subsequent free vibration of the two modes was suppressed using the self-sensing method. Figure 12 shows time histories of multiple-mode vibration suppression. Until the semi-active control started at $t = 0.16$ s, the first and second modes and the electric charge were estimated. The vibration was sufficiently suppressed in the following 0.4 s. Until $t = 0.44$ s, the self-sensing method seemed to suppress mainly the first-mode vibration, considering the time history of switching intervals. However, the second vibration mode was also suppressed well compared with natural damping alone (i.e., before $t = 0.16$ s). The self-sensing method accurately estimated the two-mode vibration, and flexibly responded to the vibration according to the relative amplitudes of the two modes.

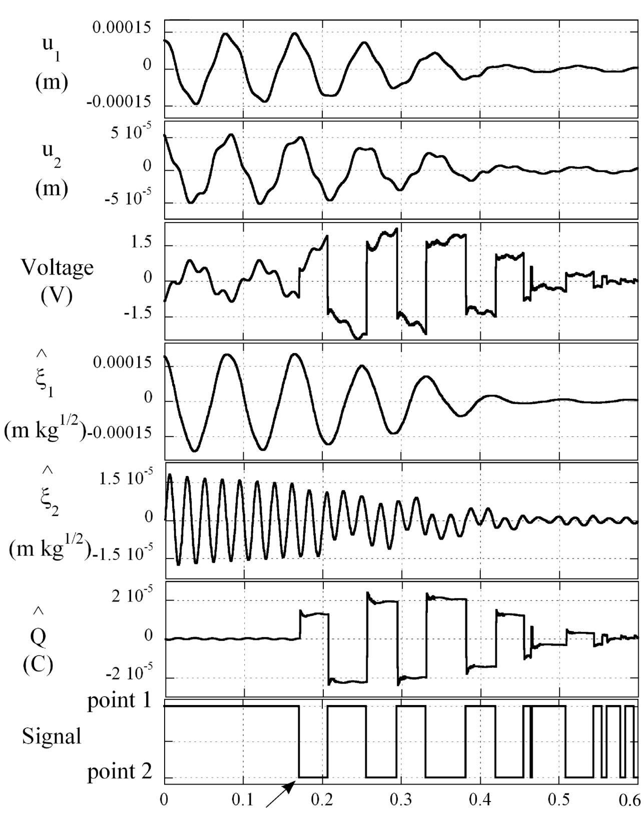

Fig. 12 Experimental result for multiple-mode vibration suppression.

V. Conclusions

This paper has discussed an innovative self-sensing method using piezoelectric actuators for energy-recycling semi-active vibration suppression. The method uses a Kalman filter for extended systems and can be applied to MDOF systems with multiple piezoelectric actuators. Insofar as demonstrated in this paper, this self-sensing method has several advantages over conventional self-sensing methods: 1) it can control multiple-mode vibration in which the vibration modes are selectively suppressed, 2) it has much lower sensitivity to residual modes, 3) it has significant robustness to parameter variations, and 4) it can control multiple piezoelectric actuators cooperatively (in the sense of the centralized-control) rather than independently.

The numerical simulations demonstrated that the self-sensing method worked well on a truss structure and had significant robustness against parameter variations. The vibration suppression experiments were also performed using a cantilevered 10-bay truss structure with the proposed self-sensing method. The experiments demonstrated that the proposed self-sensing method suppressed well not only single-mode vibration but also multiple-mode vibration of the actual structure.

This investigation evaluated the self-sensing method's performance for energy-recycling semi-active vibration suppression. However, it is clear that this self-sensing method and the results of this investigation are, in principle, applicable to other vibration suppression methods, as long as the electric current flows for a short period in a circuit connected to a piezoelectric actuator; for example, not only semi-active vibration suppression [12,13], but also hybrid active vibration suppression [26].

References

[1] Lesieutre, G. A., "Vibration Damping and Control Using Shunted Piezoelectric Materials," *Shock and Vibration Digest*, Vol. 30, No. 3, 1998, pp. 187–195.

[2] Ahmadian, M., and DeGuilio, A. P., "Recent Advances in the Use of Piezoceramics for Vibration Suppression," *Shock and Vibration Digest*, Vol. 33, No. 1, 2001, pp. 15–22.

[3] Anderson, E. H., Hagood, N. W., and Goodliffe, J. M., "Self-Sensing Piezoelectric Actuation: Analysis and Application to Controlled Structures," *Proceedings of the 33rd AIAA/ASME/ASCE/AHS/ASC Structures, Structural Dynamics and Materials Conference*, CP-2465, AIAA, Washington, DC, 1992, pp. 2141–2155.

[4] Dosch, J. J., Inman, D. J., and Garcia, E., "A Self-Sensing Piezoelectric Actuator for Collocated Control," *Journal of Intelligent Material Systems and Structures*, Vol. 3, No. 1, 1992, pp. 166–185.

[5] Tzou, H. S., and Hollkamp, J. J., "Collocated Independent Modal Control with Self-Sensing Orthogonal Piezoelectric Actuators (Theory and Experiment)," *Smart Materials and Structures*, Vol. 3, 1994, pp. 277–284.

[6] Spangler, R. L., and Hall, S. R., "Broadband Active Structural Damping Using Positive Real Compensation and Piezoelectric Simultaneous Sensing and Actuation," *Smart Materials and Structures*, Vol. 3, 1994, pp. 448–458.

[7] Carabelli, S., and Tonoli, A., "System Properties of Flexible Structures with Self-Sensing Piezoelectric Transducers," *Journal of Sound and Vibration*, Vol. 235, No. 1, 2000, pp.1–23.

[8] Clark, W. W., "Vibration Control with State-Switched Piezoelectric Materials," *Journal of Intelligent Material Systems and Structures*, Vol. 11, No. 4, 2000, pp. 263–271.

[9] Cunefare, K. A., De Rosa, S., Sadegh. N., and Larson, G., "State-Switched Absorber for Semi-Active Structural Control," *Journal of Intelligent Material Systems and Structures*, Vol. 11, No. 4, 2000, pp. 300–310.

[10] Holdhusen, M. H., and Cunefare, K. A., "Damping Effects of the State-Switched Absorber Used for Vibration Suppression," *Journal of Intelligent Material Systems and Structures*, Vol. 14, No. 9, 2003, pp. 551–561.

[11] Larson, G. D., and Cunefare, K. A., "Quarter-Cycle Switching Control for Switch-Shunted Dampers," *Journal of Vibration and Acoustics*, Vol. 126, No. 2, 2004, pp. 278–283.

[12] Richard, C., Guyomar, D., Audigier, D., and Ching, G., "Semi-Passive Damping Using Continuous Switching of a Piezoelectric Device," *Proceedings of the SPIE Smart Structures and Materials Conference*, SPIE Vol. 3672, Society of Photo-Optical Instrumentation Engineers, Bellingham, WA, 1999, pp. 104–111.

[13] Richard, C., Guyomar, D., and Audigier, D., "An Original Damping Approach using a Switched Piezoelectric Device," *Proceedings of the 10th International Conference on Adaptive Structures and Technologies*, Technomic Publishing Co., Inc., Lancaster, PA, 1999, pp. 21–28.

[14] Richard, C., Guyomar, D., Audigier, D., and Bassaler, H., "Enhanced Semi Passive Damping Using Continuous Switching of a Piezoelectric Device on an Inductor," *Proceedings of the SPIE Smart Structures and Materials Conference*, SPIE Vol. 3989, Society of Photo-Optical Instrumentation Engineers, Bellingham, WA, 2000, pp. 288–299.

[15] Corr, L. R., and Clark, W. W., "Comparison of Low Frequency Piezoceramic Shunt Techniques for Structural Damping," *Proceedings of the SPIE Smart Structures and Materials Conference*, SPIE Vol. 4331, Society of Photo-Optical Instrumentation Engineers, Bellingham, WA, 2001, pp. 262–272.

[16] Corr, L. R., and Clark, W. W., "Comparison of Low-Frequency Piezoelectric Switching Shunt Techniques for Structural Damping," *Smart Materials and Structures*, Vol. 11, 2002, pp. 370–376.

[17] Corr, L. R., and Clark, W. W., "A Novel Semi-Active Multi-Modal Vibration Control Law for a Piezoceramic Actuator," *Journal of Vibration and Acoustics*, Vol. 125, No. 2, 2003, pp. 214–222.

[18] Onoda, J., Makihara, K., and Minesugi, K., "Energy-Recycling Semi-Active Method for Vibration Suppression with Piezoelectric Transducers," *AIAA Journal*, Vol. 41, No. 4, 2003, pp. 711–719.

[19] Onoda, J., Endo, T., Tamaoki, H., and Watanabe, N., "Vibration Suppression by Variable-Stiffness Members," *AIAA Journal*, Vol. 29, No. 6, 1991, pp. 977–983.

[20] Makihara, K., Onoda, J., and Minesugi, K., "Comprehensive Assessment of Semi-Active Vibration Suppression Including Energy Analysis," *Journal of Vibration and Acoustics*, (to be published).

[21] Makihara, K., Onoda, J., and Minesugi, K., "New Approach to Semi-Active Vibration Isolation to Improve the Pointing Performance of Observation Satellites," *Smart Materials and Structures*, Vol. 15, 2006, pp. 342–350.

[22] Jaffe, B., Cook, W. R., Jr., and Jaffe, H., *Piezoelectric Ceramics*, Academic Press, London, 1971, pp. 16–20.

[23] Kwakernaak, H., and Sivan, R., *Linear Optimal Control System*, Wiley–Interscience, New York, 1972, pp. 220–222, 339–346.

[24] Makihara, K., Onoda, J., and Minesugi, K., "Behavior of Piezoelectric Transducer on Energy-Recycling Semiactive Vibration Suppression," *AIAA Journal*, Vol. 44, No. 2, 2006, pp. 411–413.

[25] Oppenheim, A. V., and Schafer, R. W., *Digital Signal Processing*, Prentice–Hall, Englewood Cliffs, NJ, 1975, pp. 148–173, 226–269.

[26] Makihara, K., Onoda, J., and Minesugi, K., "Low-Energy-Consumption Hybrid Vibration Suppression Based on an Energy-Recycling Approach," *AIAA Journal*, Vol. 43, No. 8, 2005, pp. 1706–1715.

C. Pierre
Associate Editor